A model of order-selectivity based on dynamic changes in the balance of excitation and inhibition produced by short-term synaptic plasticity

Vishwa Goudar and Dean V. Buonomano

You might find this additional info useful...

This article cites 108 articles, 66 of which can be accessed free at:
/content/113/2/509.full.html#ref-list-1

Updated information and services including high resolution figures, can be found at:
/content/113/2/509.full.html

Additional material and information about *Journal of Neurophysiology* can be found at:
http://www.the-aps.org/publications/jn

This information is current as of January 27, 2015.

A model of order-selectivity based on dynamic changes in the balance of excitation and inhibition produced by short-term synaptic plasticity

Vishwa Goudar and Dean V. Buonomano
Integrative Center for Learning and Memory, Departments of Neurobiology and Psychology, UCLA, Los Angeles, California

Goudar V, Buonomano DV. A model of order-selectivity based on dynamic changes in the balance of excitation and inhibition produced by short-term synaptic plasticity. *J Neurophysiol* 113: 509–523, 2015. First published October 22, 2014; doi:10.1152/jn.00568.2014.—Determining the order of sensory events separated by a few hundred milliseconds is critical to many forms of sensory processing, including vocalization and speech discrimination. Although many experimental studies have recorded from auditory order-sensitive and order-selective neurons, the underlying mechanisms are poorly understood. Here we demonstrate that universal properties of cortical synapses—short-term synaptic plasticity of excitatory and inhibitory synapses—are well suited for the generation of order-selective neural responses. Using computational models of canonical disynaptic circuits, we show that the dynamic changes in the balance of excitation and inhibition imposed by short-term plasticity lead to the generation of order-selective responses. Parametric analyses predict that among the forms of short-term plasticity expressed at excitatory-to-excitatory, excitatory-to-inhibitory, and inhibitory-to-excitatory synapses, the single most important contributor to order-selectivity is the paired-pulse depression of inhibitory postsynaptic potentials (IPSPs). A topographic model of the auditory cortex that incorporates short-term plasticity accounts for both context-dependent suppression and enhancement in response to paired tones. Together these results provide a framework to account for an important computational problem based on ubiquitous synaptic properties that did not yet have a clearly established computational function. Additionally, these studies suggest that disynaptic circuits represent a fundamental computational unit that is capable of processing both spatial and temporal information.

short-term synaptic plasticity; order-selectivity; context-dependent suppression and enhancement; disynaptic circuit

DISCRIMINATING THE ORDER of different sensory events is of fundamental importance to many sensory computations, including speech discrimination in humans, song discrimination in birds, echolocation in bats, as well as direction-selectivity in the visual and tactile domains (Barlow and Levick 1965; Doupe and Kuhl 1999; Hirsh 1959; Mossbridge et al. 2006; Simmons 2012). Order discrimination of phonemes, for example, is critical for speech comprehension—e.g., "de-lay" versus "la-dy" or "mi-st" versus "mi-tts". Furthermore, deficits in auditory order discrimination tasks are indicative of linguistic impairments in children (Tallal 2004; Tallal and Piercy 1973).

Consistent with the importance of temporal order discrimination in sensory processing, particularly in auditory processing, a large number of experimental studies have reported auditory order-selective neurons (also referred to as temporal-combination sensitivity) in rodents (Kilgard and Merzenich 2002; Zhou et al. 2010), cats (Brosch and Schreiner 2000), bats (Razak and Fuzessery 2009; Suga et al. 1978, 1983), songbirds (Doupe 1997; Lewicki and Arthur 1996; Margoliash and Fortune 1992), and monkeys (Bartlett and Wang 2005; Brosch et al. 1999; Sadagopan and Wang 2009; Yin et al. 2008). However, despite the behavioral relevance of stimulus order and the experimental reports of order-selective neurons, there has been relatively little emphasis on mechanistic underpinnings of order-selectivity in the auditory system.

In many of the above-mentioned neurophysiological studies, order-selectivity has been demonstrated by the presentation of pairs of stimulus features such as tones. For example, brief low (*A*)- and high (*B*)-frequency tones might be presented as pairs *AB*, *BA*, *AA*, and *BB*—where the tones are typically separated by intervals of tens to a few hundred milliseconds. Here we will define order-selective neurons as those that respond significantly more to *AB* than to *BA*, *AA*, or *BB* (or, of course, *A* or *B* by itself) (Bartlett and Wang 2005; Brosch and Schreiner 2000; Lewicki and Arthur 1996; Lewicki and Konishi 1995; Sadagopan and Wang 2009; Yin et al. 2008), whereas an *AB* order-sensitive neuron would exhibit a significantly enhanced response to *B* when it is preceded by *A* compared with its response to *B* alone (or to the linear sum *A* + *B*). From a computational perspective the formation of an *AB* order-selective neuron requires that two minimal conditions be satisfied: *1*) information from both the *A* and *B* stimuli must converge onto the selective neuron; and *2*) at some level the system must maintain a "memory" of the first tone that lasts at least until the presentation of the second tone. Thus if *A* and *B* were separated by 100 ms, there must be a "trace" of the presentation of *A* that lasts at least 100 ms. Previous models of auditory order-selectivity have satisfied both conditions by proposing that the computation relies on the convergence of information from *A* and *B* detectors, together with disinhibition of the response to *B* if it was preceded by *A* (Byrnes et al. 2011; Dehaene et al. 1987; Drew and Abbott 2003; Lewicki and Konishi 1995). Critically, however, these models have invoked customized circuits to meet these conditions. For example, some models propose the presence of recurrent circuits to keep the memory of the first sensory event "alive" until the arrival of the second event. It has also been proposed that in some systems slow ionic conductances could function as the memory trace (Hooper et al. 2002; Kanold and Manis 2005). Other auditory models invoke the existence of hardwired delays, and thus extend the concept of the Reichardt circuit, originally proposed to underlie direction-selectivity in the retina (Barlow and Levick 1965; Reichardt 1961). In the Reichardt model, direction-selectivity is achieved through postulated delays of excitatory or inhibitory inputs, which allow a neuron to respond

Address for reprint requests and other correspondence: D. V. Buonomano, Integrative Center for Learning & Memory, Depts. of Neurobiology and Psychology, UCLA, Los Angeles, CA 90095 (e-mail: dbuono@ucla.edu).

differentially to a stimulus moving in a preferred versus null direction.

Here we show that experimentally observed forms of auditory order-selectivity can emerge naturally from the known architecture of cortical feedforward disynaptic circuits and empirically derived cortical synaptic properties. Of particular importance is the presence of short-term synaptic plasticity (STP), which refers to use-dependent changes in synaptic efficacy lasting hundreds of milliseconds (Abbott and Regehr 2004; Reyes 2011; Zucker 1989; Zucker and Regehr 2002). Despite its ubiquity, the computational function of STP continues to be debated (see DISCUSSION). Our results reveal that STP is well suited to account for order-selectivity by dynamically altering the balance of excitation and inhibition. Additionally, we predict that among the different types of STP, paired-pulse depression (PPD) of inhibitory postsynaptic potentials (IPSPs) is the most important for order-selectivity.

MATERIALS AND METHODS

Simulations were implemented in the NEURON simulation environment (Hines and Carnevale 1997) and based on a previously published model (Lee and Buonomano 2012). The integration time step for all simulations was 0.1 ms.

Neuron Model

Pyramidal excitatory (Ex) and fast-spiking inhibitory (Inh) neurons were modeled as single-compartment, conductance-based leaky integrate-and-fire (IAF) units and received feedforward excitatory inputs (Inp). Here the voltage V_i of an Ex unit is described by

$$\tau_m \frac{dV_i(t)}{dt} = -\left(V_i(t) - E_L\right) + \sum_j g_{ij}^{InpEx} \cdot \left(E_{Ex} - V_i(t)\right)$$
$$+ \sum_j g_{ij}^{ExEx} \cdot \left(E_{Ex} - V_i(t)\right) + \sum_j g_{ij}^{InhEx} \cdot \left(E_{Inh} - V_i(t)\right) \qquad (1)$$

The membrane time constant, τ_m, of the Ex (Inh) units was 30 (10) ms, and the input resistance, R_{in}, was 318 (318) MΩ. Leak (E_L), excitatory (E_{Ex}), and inhibitory (E_{Inh}) reversal potentials were set to −60, 0, and −70 mV, respectively. Inh units are described similarly, except they did not receive lateral inhibition. In the experiments shown in Figs. 2, 5, 6, 7 and 8, each unit also received independent and continuous noise input in the form of a noise current, drawn from a uniform distribution in the range $[-i_{noise\_Ex}, i_{noise\_Ex}]$ ($[-i_{noise\_Inh}, i_{noise\_Inh}]$) nA. Note that in the simplified model (Figs. 1–4) there is no recurrent excitation; thus the third term on the right side of *Eq. 1* is excluded.

When spiking threshold V_{th} was reached, a spike was produced by setting the voltage to 40 mV for 1 ms. For each Ex (Inh) unit, V_{th} was drawn from a normal distribution with a −40 (−45)-mV mean and a 2 (2.25)-mV variance. A refractory period of 2 (2) ms followed an action potential, during which the voltage was set to −60 (−65) mV to turn off the spike, and was accompanied by afterhyperpolarization (AHP) with the AHP potential, E_{AHP}, set to −90 (−90) mV. The AHP conductance, g_{AHP}, was activated at spike offset, incremented by 0.22 (0.63) nS whenever a spike occurred, and decayed with a time constant of 10 (2) ms.

Synaptic Conductances and STP

Excitatory (AMPA) and inhibitory (GABA) synaptic transmission were simulated with a kinetic model as described previously (Buonomano 2000; Destexhe et al. 1994), where the AMPA (GABA) binding rate was set to 1.5 (0.5) ms^{-1}mM^{-1} and the unbinding rate to 0.75 (0.1) ms^{-1}. Synaptic delays meant to capture axonal and dendritic delays were included: 1.4 ms for Ex→Ex, 0.8 ms for Ex→Inh, and 0.6 ms for Inh→Ex synapses.

STP was incorporated at all synapses with the Tsodyks-Markram formulation (Markram et al. 1998; Tsodyks and Markram 1997). The utilization, U, depression time constant, τ_D, and facilitation time constant, τ_F, of the excitatory synapses onto postsynaptic Ex units were set to 0.4, 500 ms, and 1 ms, respectively, based on experimental data (Markram et al. 1998). STP parameters for Ex→Inh synapses were set to $U = 0.25$, $\tau_D = 300$ ms, and $\tau_F = 1$ ms (Levy and Reyes 2012; Markram et al. 1998), and for Inh→Ex synapses to $U = 0.5$, $\tau_D = 700$ ms, and $\tau_F = 10$ ms (Gupta et al. 2000; Levy and Reyes 2012).

Network Model

The default primary auditory cortex (A1) tonotopic network model was comprised of 800 Ex and 200 Inh units. The network was driven by 24 Input units, connected to the network in a deterministic and topographic manner. In the default network, each Ex unit received input from the eight Input units closest to it. At the edges of the network, these indices wrapped around to yield a circular network structure. Feedforward connections to the Inh units were generated similarly, with each Inh unit receiving projections from six of its closest Input units.

Recurrent connections were randomly generated, while statistically constraining the distance between pre- and postsynaptic units, in consideration of determinate axonal lengths. Each Ex_i received lateral excitatory projections from 50 other Ex units with indices drawn from a normal distribution with mean i and variance 10,000. Each Inh_i received lateral excitatory projections from 13 Ex units drawn from a normal distribution with mean set to the location closest to Inh_i along the Ex dimension and variance set to 10,000. Each Ex_i also received local inhibitory projections from 11 Inh units drawn from a normal distribution with mean set to the location closest to Ex_i along the Inh dimension and variance set to 90. As with the feedforward connections, recurrent connections at the edges of the network wrapped around.

Synaptic weights of each of the five classes (Input→Ex, Input→Inh, Ex→Inh, Ex→Ex, Inh→Ex) were assigned so that the Ex and Inh units responded in a robust fashion to the feedforward inputs. The lateral excitatory connections to Ex units (Ex→Ex) were not strong enough to generate self-perpetuating activity, but those to Inh units (Ex→Inh) could activate inhibitory neurons—consistent with experimental observations indicating that inhibitory neurons fire at lower stimulation intensities than excitatory neurons and receive larger excitatory postsynaptic currents (EPSCs)/potentials (EPSPs) (Carvalho and Buonomano 2009; Hull et al. 2009; Marder and Buonomano 2004; Miles 1990; Pouille and Scanziani 2001). Importantly, weights of lateral connections were calibrated to realize broader frequency tuning of the inhibitory neurons compared with excitatory neurons as observed experimentally, along with a short latency to fire (Atencio and Schreiner 2008; Li et al. 2014; Moore and Wehr 2013).

To enable tonotopically representative frequency-tuned responses in the Ex and Inh units, the absolute synaptic strengths of the feedforward connections were generated from a distance-based normal distribution function. The weight of an Input→Ex (Input→Inh) synapse with distance d_{ij} between the presynaptic unit $Input_j$ and the postsynaptic unit Ex_i (Inh_i) was determined from a distribution with mean at 0 and variance 1.5 (1.25). The absolute synaptic strength of each Input→Ex (Input→Inh) synapse was scaled by the maximal conductance 155 (66.7) nS to produce suprathreshold tonotopic responses (see Fig. 6A) and jittered between ±10%. Distances d_{ij} were calculated as the difference between the index, j, of the presynaptic unit $Input_j$ and the location along the Input dimension closest to the postsynaptic unit Ex_i (Inh_i).

The absolute synaptic strengths for recurrent synapses were drawn from normal distributions (Table 1), with mean values for the Ex→Inh

Table 1. *Distribution parameters of absolute strengths for each type of synapse*

	Mean, nS	SD, nS	Min, nS	Max, nS
Ex→Ex	1.8	1.273	0.18	
Ex→Inh	23.08	5	2.31	
Inh→Ex	25	12.5	2.5	
Input→Ex			15.5	75
Input→Inh			6.67	55

Ex, excitatory; Inh, inhibitory; SD, standard deviation.

and Inh→Ex synapses tuned for heteroenhancement. To ensure that multiple presynaptic neurons firing in close temporal proximity were collectively able to evoke a postsynaptic action potential, the absolute strengths of all excitatory synapses were bounded by the minima specified in Table 1.

Unless stated otherwise, the set of 24 Input units were modeled to correspond to a set of 8 input tones (e.g., 1–8 kHz), with 3 distinct and adjacent Input units corresponding to 1 tone: $Input_1$–$Input_3$ generated *tone 1*, $Input_4$–$Input_6$ generated *tone 2*, and so on. In Fig. 8, we examine how order-tuning varied as a function of stimulus intensity by changing the number of input units activated by each tone. For example, *tone 2* at different levels would correspond to the following inputs: *level 1*: $Input_5$; *level 2*: $Input_4$–$Input_5$; *level 3*: $Input_4$–$Input_6$; *level 4*: $Input_3$–$Input_6$; and *level 5*: $Input_3$–$Input_7$. Tone presentation at time t was simulated by a simultaneous spike at each of the corresponding Input units at time t.

Simulations for Paired-Tone Suppression and Enhancement

Analyses of the paired-tone studies (Figs. 5–8) were based on 25 trials, with noise currents injected into the Ex and Inh units. For a single trial, each Ex and Inh unit's tone response was computed as the number of spikes elicited in the unit over a 20-ms window following tone offset. In Fig. 6, enhancement/suppression of a unit in response to tone pair Tn_x→Tn_y was measured as the average difference between the unit's response to the tone Tn_y when preceded by the tone Tn_x and its response to the tone Tn_y by itself. Network simulations in Fig. 7 and Fig. 8 were executed on five network replications (25 trials each), each generated with a different random seed. Results presented in these figures represent means over these replications, with error bars measuring SE.

Order selectivity. In the large-scale network simulations (Fig. 7 and Fig. 8), units were classified as experiencing enhancement (suppression) to tone pair Tn_x→Tn_y if the number of spikes elicited by tone Tn_y when preceded by tone Tn_x was statistically greater (less) than that elicited by tone Tn_y alone (χ^2-test, $P \leq 0.01$). Similarly, units were classified as order-selective to tone pair Tn_x→Tn_y if the number of spikes elicited by tone Tn_y when preceded by tone Tn_x was statistically greater than that elicited by tone Tn_x alone, Tn_y alone, Tn_x when preceded by Tn_x, Tn_x when preceded by Tn_y, and Tn_y when preceded by Tn_y (χ^2-test, $P \leq 0.01$). One-way analyses of variance (ANOVAs) were performed to characterize the impact of τ_D of the Inh→Ex synapses on the prevalence of order-selective, enhanced, and suppressed responses.

Quantification of heteroenhancement and homosuppression. Two-way ANOVAs were performed to measure the impact of τ_D of the Inh→Ex synapses on the extent to which heteroenhancement and homosuppression were observed in units exhibiting these responses.

RESULTS

STP of Input→Ex, Input→Inh, and Inh→Ex Synapses

To determine whether order-selectivity can arise from simple circuits with empirically derived forms of short-term plas-

ticity we first simulated a reduced disynaptic circuit composed of a single Ex and a single Inh neuron that receive a shared excitatory input (Input), where the Inh neuron synapses onto the Ex neuron (Fig. 1*A*). These feedforward disynaptic circuits are universally present in cortical networks and may represent a fundamental computational unit (Shepherd 1998; Silberberg and Markram 2007). Disynaptic circuits have at least three distinct synapse classes: Input→Ex, Input→Inh, and Inh→Ex. Although often overlooked in computational models, each of these synapse classes exhibits unique and robust forms of STP. Because the dynamic changes in the balance of excitation/inhibition imposed by STP will be critical to the present model's ability to exhibit order-sensitivity, it is necessary to first describe the different forms of STP at each synapse class.

Experimental studies reveal that STP at each of these three synapse classes varies significantly in terms of direction, magnitude, and time course, but they nevertheless exhibit characteristic signatures. The Inh→Ex connection of our simplified circuit potentially represents multiple synapse classes because of the diversity of inhibitory neurons in the cortex. Here we focus primarily on disynaptic circuits in which the Inh neuron represents fast-spiking/parvalbumin-positive inhibitory neurons because *1*) they are the most common subtype of inhibitory neuron and *2*) precisely because they are fast spiking, they play a more prominent role in feedforward circuits and the gating of short-lasting stimuli (Carvalho and Buonomano 2009; Kawaguchi and Kubota 1997; Reyes 2011; Rudy et al. 2011). Multiple studies have demonstrated that IPSPs from parvalbumin-positive inhibitory neurons onto excitatory neurons undergo robust PPD on a timescale of hundreds of milliseconds (Gupta et al. 2000; Kapfer et al. 2007; Ma et al. 2012; Reyes 2011)—in contrast, IPSPs from low-threshold somatostatin-positive inhibitory neurons are primarily facilitating. Indeed, before the now standard distinction between parvalbumin and somatostatin inhibitory neurons was made, IPSPs were generally characterized as undergoing PPD (Buonomano and Merzenich 1998; Deisz 1999; Lambert and Wilson 1994; Metherate and Ashe 1994; Nathan and Lambert 1991), presumably because parvalbumin-positive inhibitory neurons represent >50% of the inhibitory neurons in the cortex (Gonchar and Burkhalter 1997; Kubota et al. 2012).

In our reduced disynaptic circuit, the shared excitatory input to the Ex and Inh neurons could represent either thalamocortical or cortico-cortical connections. Although there are significant differences between these two inputs, they generally exhibit similar forms of STP. Excitatory synapses onto fast-spiking inhibitory neurons (Input→Inh) have mostly been reported to undergo PPD (Gabernet et al. 2005; Levy and Reyes 2012; Lu et al. 2007; Kapfer et al. 2007; Reyes 2011). STP of the Input→Ex synapses are more variable and exhibit robust PPD to mild facilitation (Cheetham et al. 2007; Gabernet et al. 2005; Reyes and Sakmann 1999; Wang et al. 2012). It is important to note that STP at these synapses may be variable because it is modified in an experience-dependent fashion (see DISCUSSION; Carvalho and Buonomano 2011; Cheetham and Fox 2011; Finnerty and Connors 2000).

On the basis of the experimental data cited above we simulated STP in the three synaptic classes, using the Tsodyks formulation of STP (Markram et al. 1998; Tsodyks and Markram 1997). In this model, STP is governed by three parameters: U, τ_D, and τ_F. U reflects the fraction of available
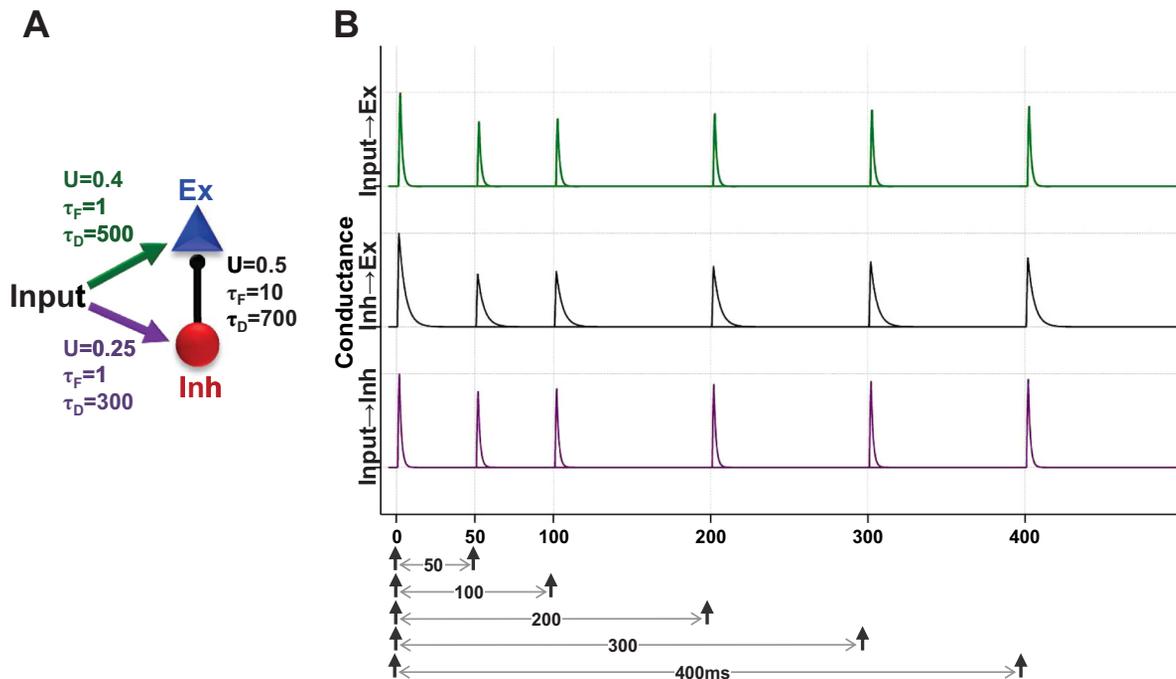
Fig. 1. Simulation of short-term synaptic plasticity (STP) at the 3 synapse classes of a disynaptic circuit. *A*: a reduced canonical disynaptic circuit composed of an Input, excitatory (Ex) and inhibitory (Inh) units, and 3 synapse classes [Input→Ex, Input→Inh, and Inh→Ex (green, purple, and black, respectively)]. STP at each synapse is captured by 3 parameters: utilization (*U*) and the facilitation (τ_F) and depression (τ_D) time constants (ms). *B*: sample synaptic conductance traces demonstrating the profile of STP at the 3 synapse classes. The traces correspond to the parameters shown in *A* and were based on experimental data (see MATERIALS AND METHODS). Overlaid paired-pulse plasticity traces in response to 5 different interstimulus intervals (ISIs) are shown (dashed lines show peak of conductance in response to 1st input). All synapse classes are depressing and exhibit stronger depression in response to shorter ISIs.

transmitter released (and can be also be thought of as approximating release probability). τ_D and τ_F are the time constants that govern the time course of synaptic depression and facilitation, respectively. Together, these three variables can be used to fit a wide range of different flavors of STP. Figure 1*B* provides an example of STP at the three different synapse classes: the Input→Ex and Input→Inh synapses exhibited mild PPD, while the Inh→Ex synapse exhibited robust PPD. The values of *U*, τ_D, and τ_F were based on published values or estimates from experimental data (Gupta et al. 2000; Levy and Reyes 2012; Markram et al. 1998). However, as described below, we performed parametric analyses to examine the dependence of our results on the STP signatures.

Order-Selectivity in a Canonical Disynaptic Circuit with STP

Having constructed a disynaptic circuit model that captures the experimentally observed forms of STP at each synapse, we next examined whether such circuits exhibit order-selectivity. Figure 2*A* illustrates a circuit driven by two inputs that can be thought of as representing two brief tones, *A* and *B*, of different frequencies. These tones create four stimuli pairs (*AA*, *AB*, *BA*, and *BB*). In this example, the interval between the tones in a pair was 100 ms. Figure 2*B* illustrates a case of order-selectivity where the Ex unit responds to *AB* but not to *AA*, *BB*, or *BA*. That is, it responds to *B* preceded by *A* but not to *B* alone (first tone of *BB* or *BA* pair) or to *B* preceded by *B*. *AB* selectivity arises as a result of a strong excitatory input from *B* (Input$_B$→Ex), which can provide a suprathreshold EPSP to Ex; however, as is often observed experimentally, this EPSP is masked ("vetoed") by the IPSP also elicited by *B*—which is

why Ex does not respond to a solitary *B* stimulus. However, the strong Input$_B$→Ex connection is not vetoed by the inhibitory neuron if *B* was preceded by *A* because of the characteristic PPD of IPSPs. In other words, *A* shifts the balance of excitation/inhibition received by Ex when it precedes *B*, resulting in a spike. Note that the presentation of *BB* also produces depression of the IPSPs in this simple circuit; however, Ex does not fire to *BB* because of the parallel depression of the Input$_B$→Ex synapse.

Interestingly, weakening the short-term depression in the Input→Ex synapses and the weight of the Input$_A$→Inh synapse can transform the disynaptic circuit in Fig. 2*A* to one that produces a *BB*-selective neuron (data not shown). In this case, a response to *AB* is precluded because *A* no longer drives Inh and thus does not disinhibit Ex's response to *B*. *BB* selectivity then arises from the response to *B* when preceded by another *B* owing to the disinhibition produced by the strong PPD of the IPSP (despite a small amount of PPD in the Input$_B$→Ex synapse).

It is important to highlight that the above mechanisms rely on an experimentally well-characterized property of cortical disynaptic circuits: even though the disynaptic route taken by the IPSP delays it relative to the EPSP, it is still rapid enough to "veto" a suprathreshold monosynaptic Input→Ex EPSP. Specifically, disynaptic IPSPs interact with the rising slope of monosynaptic EPSPs and can prevent suprathreshold EPSPs from producing a spike (Carvalho and Buonomano 2009; Daw et al. 2007; Marder and Buonomano 2004; McCormick et al. 1993; Pouille and Scanziani 2001). In fact, cortical circuits seem to be "designed" precisely to allow fast-spiking/parvalbumin-positive inhibitory neurons to implement this computa-
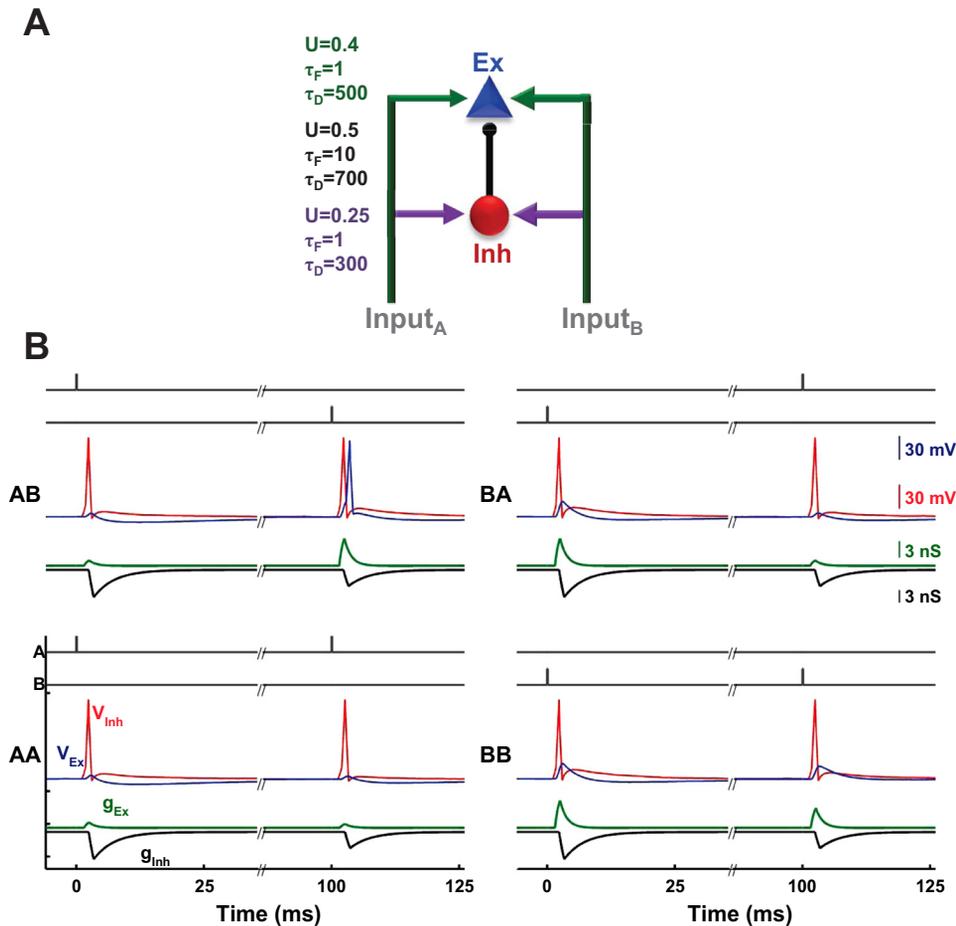
Fig. 2. Example of order-selectivity in a reduced disynaptic circuit. *A*: a canonical disynaptic circuit with 2 inputs that exhibits strong *AB* order-selectivity. Each synapse class is accompanied by the values of its STP parameters. The weights of the Input$_A$→Ex, Input$_B$→Ex, Input$_A$→Inh, Input$_B$→Inh, and Inh→Ex synapses were set to 3, 15, 9, 12 and 33 nS, respectively. *B*: mechanisms of order-selectivity. Representative voltage traces for the Ex (blue) and Inh (red) units, and excitatory (green) and inhibitory (black) conductance traces of the Ex unit, in response to each of the 4 stimuli pairs (*AB*, *BA*, *AA*, and *BB*; 100-ms ISI). Conductance traces illustrate the dynamic changes in the balance of excitation-inhibition induced by STP, which gives rise to *AB* order-selectivity. Depression of the inhibitory postsynaptic current (IPSC) results in a context-dependent response of the Ex unit to *B* only when preceded by *A*. Importantly, during *BB* stimulation, the first *B* does not disinhibit a response to the second *B* because of paired-pulse depression (PPD) of the Input→Ex EPSC. The Ex (Inh) unit received noise input with i_{noise_Ex} (i_{noise_Inh}) set to 0.001 nA (0.001 nA).

tional feature: fast-spiking inhibitory neurons synapse on the cell soma or proximal dendrites of pyramidal neurons, receive large-amplitude EPSPs, and have time constants that are often half those of pyramidal neurons (Daw et al. 2007; Holmgren et al. 2003; Hull et al. 2009; Levy and Reyes 2012; McCormick et al. 1985).

It should also be noted that even in the simple disynaptic circuit described in Fig. 2, there can be additional mechanisms contributing to order-selectivity. For example, the effects of subtle shifts in the latency of the firing of the Inh neuron produced by STP of the Input→Inh synapse can also contribute. Based on this mechanism it is possible to switch between an *AB*-selective and a *BB*-selective unit by only changing synaptic weights (data not shown). This mechanism, however, is not as robust as that achieved by also changing short-term depression in the Input→Ex synapses.

Order-selectivity, by definition, requires a short-lasting "memory" that enables the first sensory event to influence the response to the second. The simple model described above demonstrates that the "memory" that bridges the presentation of the two distinct stimulus events can be implemented by STP.

PPD of IPSPs Is the Most Important Form of STP for Order-Selectivity

The above results establish that a disynaptic circuit composed of a single Ex and a single Inh neuron can generate order-selectivity when the synapses exhibit STP. While the STP parameters in the above simulations were empirically derived, the synaptic weights were hand-tuned to generate order-selectivity. Thus the results do not address the more difficult questions of how dependent order-selectivity is on the parameters of the model, and whether one form of STP is more important for order-selectivity than the others.

To address these questions we performed a parametric analysis of order-selectivity in the disynaptic circuit. Even a simple two-neuron disynaptic circuit, however, has a significant number of free variables: 5 synaptic weights and the 3 parameters that govern STP (U, τ_D, and τ_F) in each of the 3 synapse classes, for a total of 14 parameters. Because we are focusing primarily on cases in which only two events are being used, the STP parameters τ_D and τ_F are sufficient to capture most regimes of STP, reducing the parameter space to 11 dimensions. Additionally, because of the inherent symmetry between stating that a cell is *AB* or *BA* order-selective, we limit our exploration of the parameter space for regions that produce *AB* selectivity. In keeping with this constraint, we can fix the Input$_A$→Ex weight at a low value (because *AB* selectivity requires that the Ex unit not fire in response to *A* by itself). Thus, for the purposes of performing a parametric analysis, the parameter space can be reduced to a total of 10 dimensions (4 weights + 6 STP parameters; we are assuming the STP parameters at different synapses within the same class are the same). Although large, this dimensionality is tractable enough for a coarse parametric analysis. We explored this parameter space by varying the synaptic weights over 7 values and each of the STP parameters over 4 values for a total of 9,834,496

$(7^4 \times 4^6)$ points. For each point we presented all four stimuli pairs (in the absence of noise) and classified each point in parameter space as leading to selectivity if the Ex unit only responded to the *AB* stimulus.

Figure 3 illustrates this approach in a simple two-dimensional parametric analysis (weight and τ_D of the Inh→Ex synapse—7×4 parameter sets) while holding the other eight parameters at the values used in Fig. 2. One can visualize which of the 28 points in the parameter space generated order-selectivity by the presence of a spike in the blue voltage trace (response to *AB* stimulus) and absence of spikes in the magenta voltage traces (responses to *BA*, *AA*, and *BB* pairs). The traces corresponding to these points are highlighted in gray. As can be seen, when the Inh→Ex synapse is relatively weak, the IPSPs in Ex are insufficient to mask the EPSPs from either stimulus of any stimuli pair. On the other axis, smaller values of τ_D yield weak disinhibition in response to the second stimulus of each pair, resulting in a circuit that is incapable of robustly producing an order-selective response. Order-selectivity is more robust in a subspace of the parameter space where the Inh→Ex weight is strong, and there is significant PPD of the IPSP.

Our analysis of the full 10-dimensional parameter space (Fig. 4) is greatly simplified by focusing on each dimension in isolation and asking whether for every value in that dimension there was a region of the remaining subspaces that led to order-selectivity. If so, we asked how large (number of points) this region was. This approach would reveal that a given parameter value is *1*) necessary for order-selectivity, if order-selectivity is only observed in regions of subspaces containing that value, and *2*) sufficient for order-selectivity, if this region spans the entire corresponding subspace. For example, the τ_F dimension for the Input→Ex synapses was set to 1, 200, 400, and 700, and for each one of these values there were a corresponding 2,458,624 ($7^4 \times 4^5$) parameter combinations (combined from the remaining 9 dimensions) spanning the corresponding subspaces. Of these, there were a total of 185,685, 96,438, 64,984, and 48,220 parameter combinations, corresponding to each value of τ_F, which generated *AB* selec-

tivity (green line in Fig. 4*B*, *right*). Thus it is clear that, regardless of whether the Input→Ex synapses exhibit no facilitation ($\tau_F = 1$) or long-lasting facilitation ($\tau_F = 700$ ms), order-selectivity can be robustly achieved. This leads to the conclusion that paired-pulse facilitation (PPF) of the Input →Ex synapses is not necessary (or sufficient) for order-selectivity—which of course does not imply that it does contribute to order-selectivity in some regions of parameter space. As shown in Fig. 4, the only STP parameter that had a value that did not produce order-selectivity in any region of the remaining parametric subspace was τ_D of the Inh→Ex synapse. Specifically, for τ_D values of 1, 200, 400, and 700 there were 0, 68,494, 138,698, and 188,135 points in the corresponding subspaces that admitted order-selectivity, respectively. Thus in the absence of PPD of the IPSP ($\tau_D = 1$) order-selectivity was not observed in any region of parameter space. Furthermore, Fig. 4*C* provides a 2-dimensional (while the other 8 parameters are held constant) subsample of the results of the 10-dimensional analysis for visualization purposes. The figure reveals that, as expected, a large portion of the explored subspace responds to *B* (*B* and *AB*, magenta). Robust order-selectivity was observed over a parameter range in which the Input$_B$→Inh and Input$_B$→Ex synaptic weights were balanced (diagonal red area). The results of this comprehensive high-dimensional parametric study, together with our conceptual understanding of the disynaptic circuit, allow us to conclude that *1*) PPD of the IPSPs is necessary (but not sufficient) for order-selectivity and *2*) order-selectivity is observed over a wide range of different parameter values, albeit with nonlinear interactions between the parameters.

Order-Selectivity in a Network Model of A1

The above results in a reduced disynaptic circuit establish that the dynamic shift in the balance of excitation and inhibition produced by STP can underlie order-selectivity. However, our proposal is not that order-selective neurons arise by customizing the weights within isolated disynaptic circuits but rather that, as explored next, subpopulations of neurons that
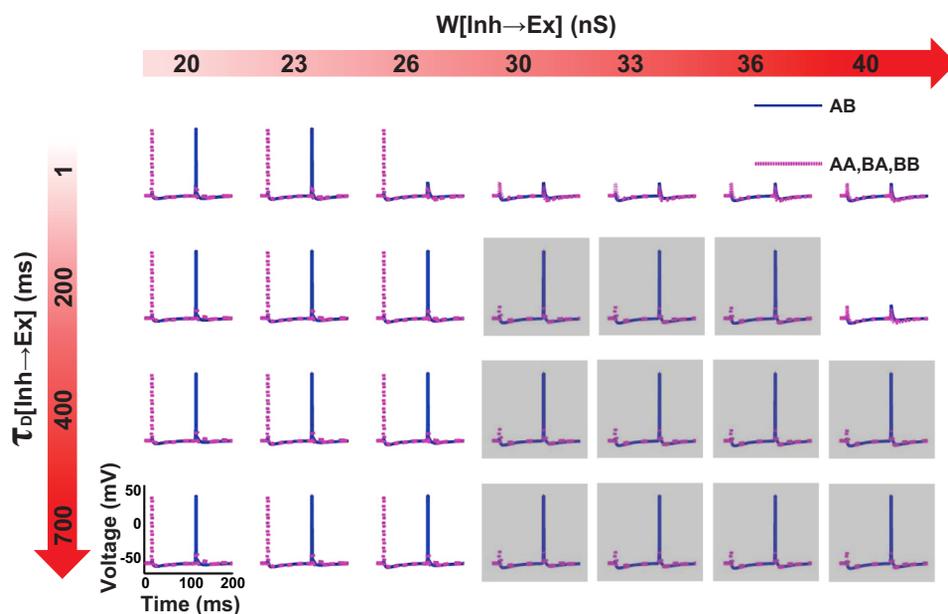
Fig. 3. Schematic of a 2-dimensional parametric analysis of order-selectivity. Simplified example of the 10-dimensional parametric analysis with 2 dimensions. The weight (*W*) and τ_D values of the Inh→Ex synapse were parametrically varied over 7 and 4 values (*x*- and *y*-axes, respectively). All other STP parameters and synaptic weights were held constant at values corresponding to those in Fig. 2. Each subpanel shows the overlaid voltage trace of the Ex unit in response to the 4 stimuli (*AA*, *BA*, *BB* in magenta and *AB* in blue; 100-ms ISI). *AB* order-selectivity can be seen by the presence of a blue spike in response to the 2nd stimulus and the absence of any magenta spikes (subpanels shaded in gray).

A

	# of Values of Parameters		
Synapses	**W**	**τ_D**	**τ_F**
Input$_A$→Inh	7	4	4
Input$_B$→Inh	7		
Input$_B$→Ex	7	4	4
Inh→Ex	7	4	4

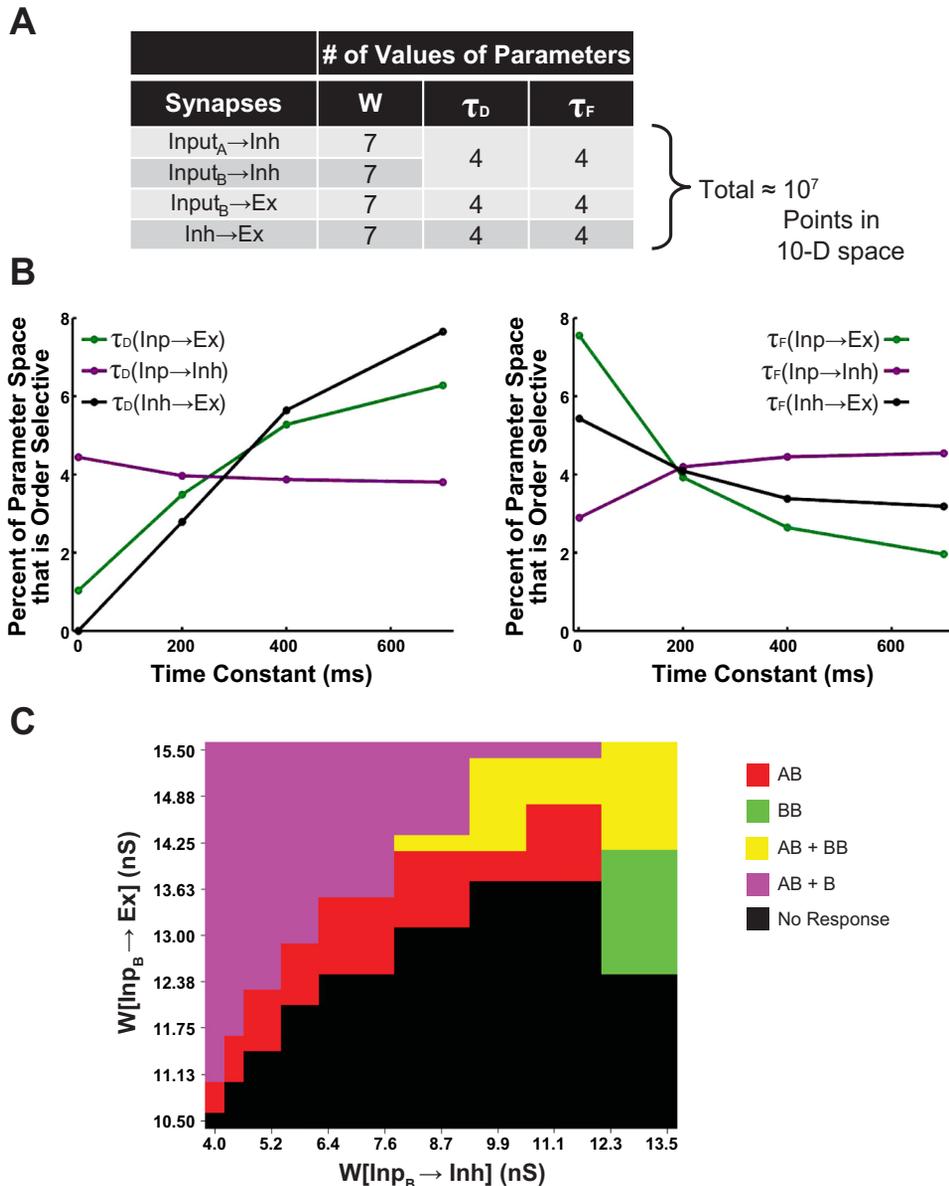Total ≈ 10^7 Points in 10-D space

B

C

Fig. 4. Ten-dimensional parametric analysis reveals that PPD of the inhibitory postsynaptic potential (IPSP) is the most important parameter for order-selectivity. *A*: table of the parameter space over which coarse parametric analysis was conducted. The weights of the Input$_A$→Inh, Input$_B$→Inh, Input$_B$→Ex, and Inh→Ex synapses were varied over 7 values, and the STP time constants of these synapses over 4 values, for a total of ~10^7 points in parameter space. *B*: % of parametric subspaces identified as order-selective as a function of the depression (*left*) and facilitation (*right*) time constants in each of the 3 synapse classes. For each dimension, results were quantified by the proportion of the related parametric subspaces that resulted in order-selective responses. For example, the black curve in the plot on *left* shows % of the parameter space, for each value of τ_D of the Inh→Ex synapse, in which *AB* selectivity occurred (collapsing across the other 9 dimensions). The robustness of order-selectivity increases with short-term depression (higher τ_D) in the Input→Ex and Inh→Ex synapses. Conversely, order-selectivity robustness decreases as the short-term facilitation of Input→Ex and Inh→Ex increases. Importantly, the only parameter with a value that did not result in any order-selectivity was the short-term depression of Inh→Ex synapse. *C*: selectivity map across a plane of the 10-dimensional parametric space spanning the Input$_B$→Inh and Input$_B$→Ex synapse weights (*W*). The plane corresponds to τ_F values of 1 ms, 700 ms, and 1 ms and τ_D values of 1 ms, 1 ms, and 700 ms for the Input→Ex, Input→Inh, and Inh→Ex synapses, respectively, and *W* values of 3 nS, 8 nS, and 30 nS for the Input$_A$→Ex, Input$_A$→Inh, and Inh→Ex synapses, respectively. Areas in red (green) represent regions of the *W*[Input$_B$→Inh]-*W*[Input$_B$→Ex] plane that are *AB* (*BB*) selective. Yellow areas correspond to regions eliciting order-sensitive responses to *AB* and *BB*, while magenta areas correspond to regions eliciting responses to *B* by itself and order-sensitive responses to *AB*. Black areas correspond to regions that elicit no response to any of the stimuli.

exhibit order-selectivity arise naturally from large neural networks with STP because of the inherent variability and richness of connectivity patterns and weights within cortical circuits.

In vivo electrophysiological studies in the auditory cortex have reported a wide range of response properties to tone-pair presentations, including forward masking, enhancement, and order-selective responses. Forward masking, or suppression, refers to the situations in which a neuron responds less to a test tone when it is preceded by another tone compared with the test tone alone (Brosch and Schreiner 1997; Scholes et al. 2011; Wehr and Zador 2005). Forward masking is most predominant when the tone pairs are of the same frequency (which we will refer to as "homosuppression") and separated by short intervals (<50 ms). Paired-tone enhancement and order-selectivity have also been reported in numerous studies (Brosch et al. 1999; Brosch and Schreiner 2000; Kilgard and Merzenich 2002; Sadagopan and Wang 2009; Yin et al. 2008). In these studies, the response to a single test tone may be small or absent when

presented alone but enhanced when it follows a conditioning tone. Enhancement is more prevalent when the conditioning tone (the first of the pair) is different but within an octave of the test tone ("heteroenhancement"). Note that while neurons responding with enhancement are order-sensitive, they are not necessarily order-selective, because an order-sensitive neuron might also respond to a tone by itself, or to some other pairing of tones. We next determined whether the incorporation of empirically derived forms of STP into a simple topographic network model of the A1 can account for these experimental observations.

The A1 model was composed of 800 excitatory and 200 inhibitory IAF units. A circuit property incorporated into the simulation was that the frequency tuning of the inhibitory neurons was broader than that of the excitatory neurons and that the inhibitory units exhibited shorter spike latencies (Atencio and Schreiner 2008; Li et al. 2014; Moore and Wehr 2013). A number of studies have suggested that excitatory and inhibitory responses in A1 are co-tuned (Tan et al. 2004; Wehr and

Zador 2003); however, it remains an open issue whether the width of the frequency tuning is broader in fast-spiking (parvalbumin positive) inhibitory neurons than in pyramidal neurons or not (Atencio and Schreiner 2008; Li et al. 2014; Moore and Wehr 2013). Inputs to the A1 model represent L-IV neurons and were topographically arranged to generate the characteristic tonotopicity of A1 (see MATERIALS AND METHODS). The Ex units represent L-II/III pyramidal neurons, and as such project "horizontally" to neighboring excitatory and inhibitory units (see MATERIALS AND METHODS). The STP parameters were guided by in vitro experimental data and were the same as those used in the disynaptic circuit above (Fig. 2).

Figure 5A, left, displays the neurogram of the entire network in response to a 5-kHz tone followed 100 ms later by a 4-kHz tone (Tn5→100→Tn4), and Fig. 5A, right, displays the response to a Tn4→100→Tn4 stimulus. The critical question relates to the response properties of the units when presented with paired tones, and particularly whether paired-tone suppression and/or enhancement, as well as order-selectivity, is observed. There was a large diversity of neural responses to paired tones, including units that spiked in response to the "anatomically" defined characteristic frequency (CF) independently of the preceding stimulus, units that were suppressed by a preceding tone of the same frequency, and order-sensitive units that responded more robustly to their "CF" when it was preceded by a conditioning tone. Example voltage traces for each of these types of units are shown in Fig. 5B.

To quantify the overall behavior of the network we first plotted the spike count of each Ex unit in response to the eight distinct input tones presented individually (Fig. 6A). Responses to single tones demonstrated a characteristic tonotopic activation of the network. Next we quantified the interactions of paired tones separated by intervals of 25–200 ms, by plotting whether the spike count response of each Ex unit to a tone was suppressed or enhanced by preceding tones. Figure 6B depicts these interactions for the case in which the test tone was Tn4 and the conditioning tone was varied between Tn1 and Tn8. The red lines on row Tn4 in Fig. 6B, middle (100-ms interval), illustrate the forward masking produced by a preceding Tn4 presentation (the "homotone" condition), while the blue lines on rows Tn3 and Tn5 reflect units that fired exclusively (order-selectivity) or more (enhancement) to Tn4 when preceded by the tone of the corresponding row ("heterotone" conditions). At short interstimulus intervals (ISIs), the predominance of red lines indicates that the great majority of neurons with Tn4 CFs were suppressed by preceding tones in the range of Tn1–Tn7 (Fig. 6B, top). At longer ISIs, enhancement was observed in ~60–70% of the subpopulation of units that received direct input from Tn4 (Fig. 6B, middle and bottom). However, enhancement was weaker at a 200-ms ISI than at a 100-ms ISI. Consistent with experimental data, this order-sensitivity was primarily observed when the preceding tone was immediately adjacent to the CF (heteroenhancement), e.g., Tn3→100→Tn4 or Tn5→100→Tn4, whereas suppression was most prominent in response to paired tones presented at the same frequency (homosuppression), e.g., Tn4→100→Tn4.

The global suppression observed at an ISI of 25 ms is produced primarily by the ongoing IPSP. However, the Input→Ex PPD also contributes to the homosuppression (e.g., Tn4→25→Tn4). The moderate homosuppression at longer intervals is predominantly produced by PPD of the Input→Ex

synapses. As in the disynaptic circuits above, order-sensitivity (blue units in Fig. 6B) requires both the convergence of different input tones onto the Inh units and PPD of IPSPs. Consider the Tn5→100→Tn4-sensitive Ex unit 373 in Fig. 5B. This unit responds weakly to Tn4 by itself, but anatomically Tn4 is its CF because it receives strongest direct inputs from Tn4—both excitatory and inhibitory. In addition, inhibitory units neighboring Ex unit 373 are also activated by Tn5 as a result of direct input from Tn5 and strong lateral projections from Ex units within the anatomical Tn5 zone (see MATERIALS AND METHODS). Because Tn5 activates some of the same Inh neurons neighboring Ex unit 373 as Tn4, the IPSPs that would normally veto a spike in Ex unit 373 in response to Tn4 by itself are depressed when Tn4 is preceded by Tn5, making the unit Tn5→Tn4 sensitive.

The quantitative results above are, of course, somewhat dependent on the network's parameters. Of particular importance are the magnitudes of STP and the average strengths of the Input→Ex and Inh→Ex synapses. Altering these parameters can change the relative dominance and time course of enhancement or suppression. For example, in the model it is easy to shift to a regime that is dominated by homosuppression and exhibits little order-sensitivity, by decreasing the PPD of IPSPs. Thus a prediction that arises is that differences between experimental findings, in terms of the relative number of neurons that exhibit either homosuppression or heteroenhancement, likely reflect not only species or experimental differences but also experience-dependent differences that alter the relative tuning of the cortical networks to favor one regime over another (Engineer et al. 2008; Kilgard and Merzenich 2002; Zhou et al. 2010). Specifically, experience-dependent increases in the percentage of neurons that exhibit order-sensitive responses, as opposed to forward suppression, could be a result of long-term changes in the magnitude and temporal profiles of STP.

To evaluate this possibility, we varied τ_D of the Inh→Ex synapses between 1 ms (no PPD) and 700 ms and measured the prevalence and extent of order-selectivity, heteroenhancement, and homosuppression in response to paired tones with a 100-ms ISI (Fig. 7). As would be expected, the population's response to single tone presentations was nearly identical across values of τ_D (Fig. 7A; $F_{3,16} < 0.01$, $P = 1$; n refers to network replications), because τ_D does not affect the IPSP in response to the first tone. However, Fig. 7B shows that the percentage of units exhibiting order-selectivity (see MATERIALS AND METHODS for the quantification of order-selectivity) and heteroenhancement increased with the PPD of the IPSPs (order-selectivity, $F_{3,16} = 252$, $P < 10^{-10}$; heteroenhancement, $F_{3,16} = 2,892$, $P < 10^{-10}$), while the percentage of units exhibiting homosuppression decreased ($F_{3,16} = 1,516$, $P < 10^{-10}$). Increasing the PPD of the IPSPs increases the magnitude of disinhibition in response to the second tone, making it easier to elicit an enhanced response to a second heterotone and more difficult to elicit a suppressed response to a second homotone. We also quantified the magnitude of enhancement and suppression among the subset of enhanced and suppressed cells, respectively. In keeping with our prediction, Fig. 7C shows that heteroenhancement increased with the PPD of the IPSPs (significant interaction between τ_D[Inh→Ex] and enhancement, $F_{2,24} = 8.32$, $P = 0.0018$). This indicates that strengthening of the PPD of the IPSPs increases not only the
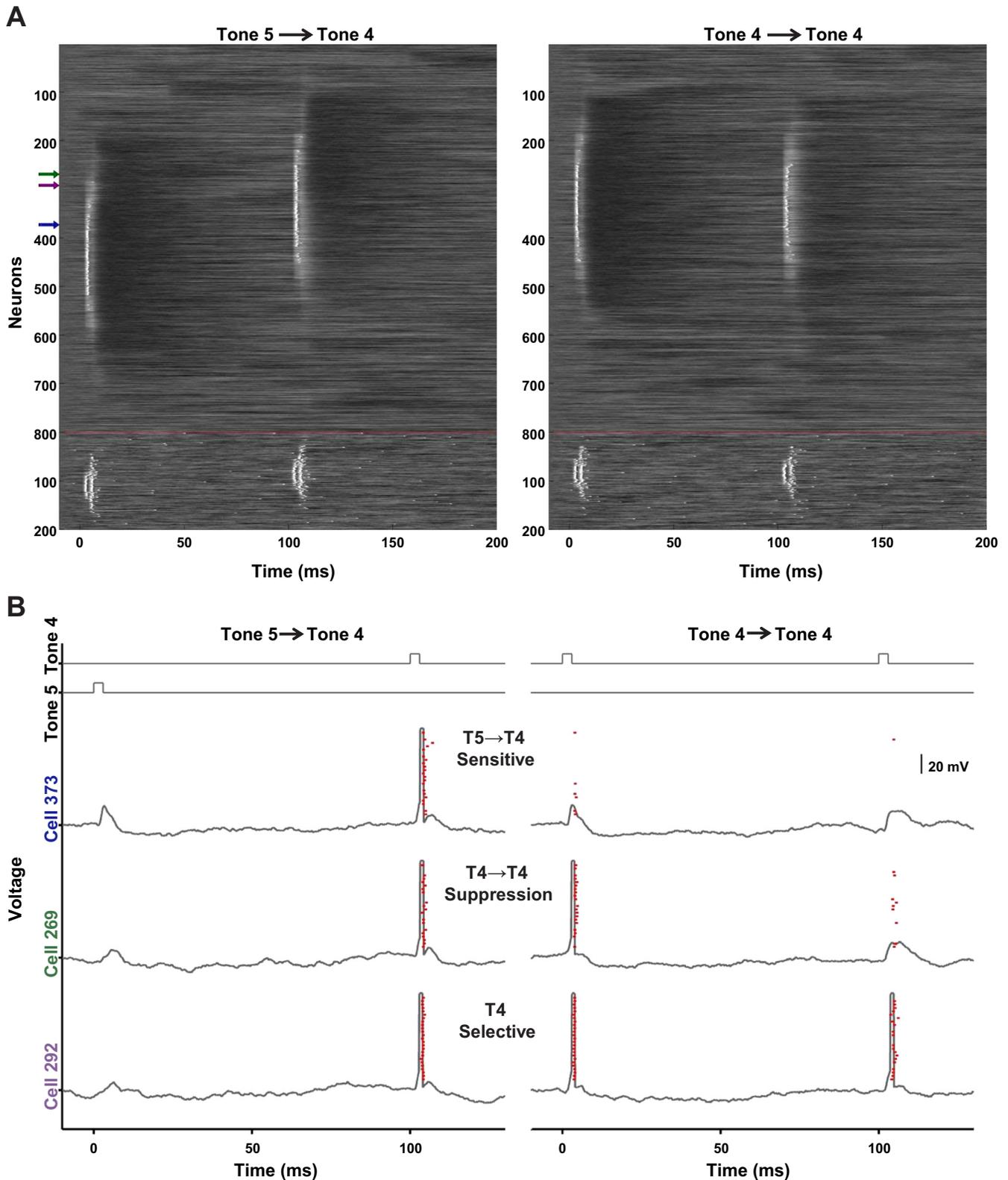
Fig. 5. Responses of a tonotopic network model of primary auditory cortex (A1) to paired tones. *A*: single-trial voltagegram of the entire 1,000-unit tonotopic network model in response to *tone 5* followed 100 ms later by *tone 4* (Tn5→100→Tn4; *left*) and Tn4→100→Tn4 (*right*). *Units 1–800* (*top*) correspond to the topographically ordered Ex units, while *units 1–200* (*bottom*) correspond to the topographically ordered Inh units. Each Ex (Inh) unit received independent noise input with i_{noise_Ex} (i_{noise_Inh}) set to 0.04 nA (0.025 nA). *B*: voltage traces for 3 Ex units, selected from *A*, indicating the diversity of neural responses observed to paired tones. The response of Ex *cell 373* (*top*) provides an example of an order-sensitive response to Tn5→100→Tn4. Similarly, the responses of *cells 269* (*middle*) and *292* (*bottom*) correspond to forward suppression and a strong response to the characteristic frequency (CF) independent of the preceding stimulus, respectively. The location of each of these units is denoted by an arrow in *A* colored to match the label of the corresponding unit in *B*. Red dots overlying the voltage traces represent spiking responses over 25 trials in order to visualize the trial-to-trial variability.
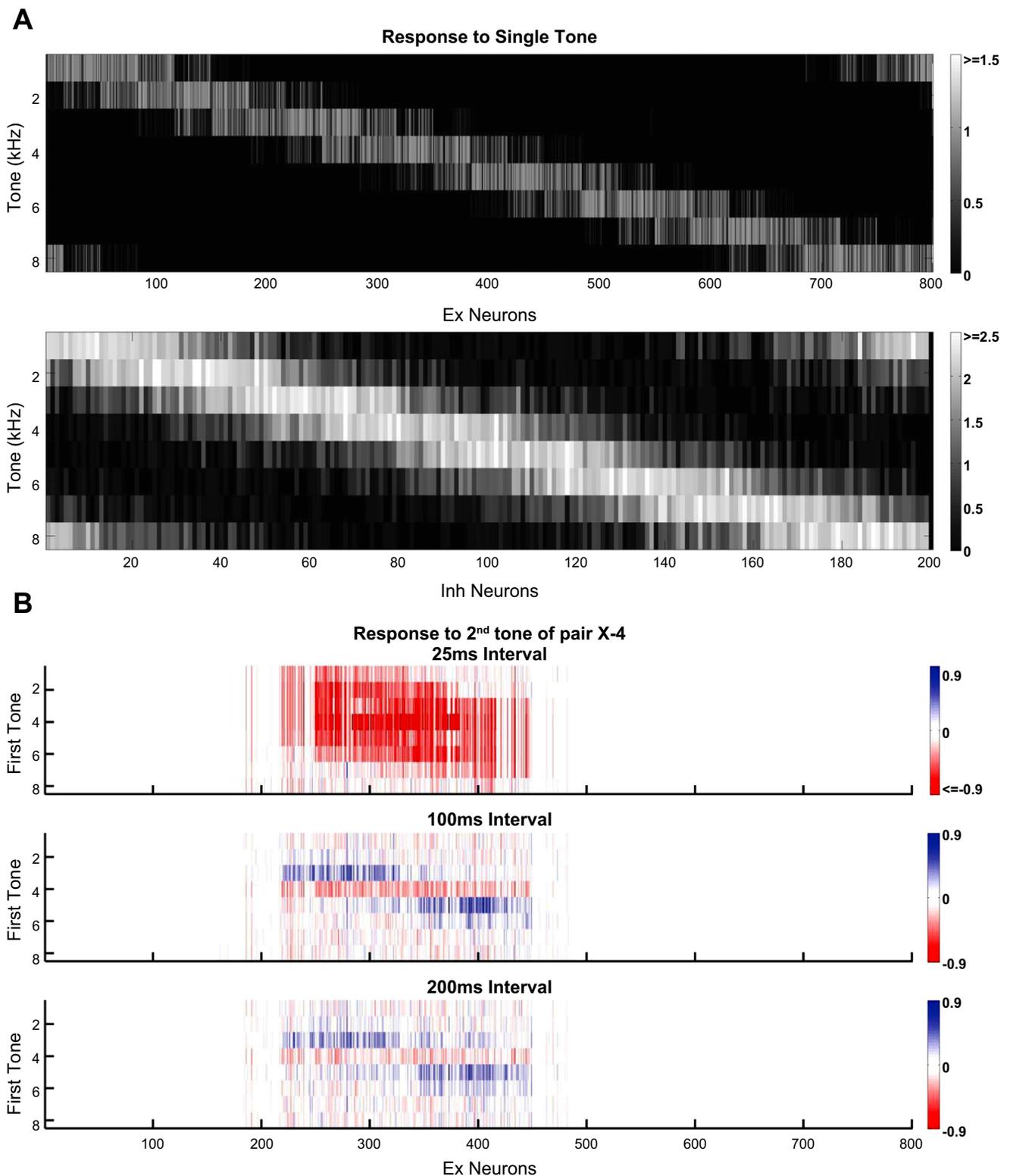
Fig. 6. Paired-tone enhancement and suppression in the tonotopic A1 model. *A*: responses of all Ex (*top*) and Inh (*bottom*) units comprising the network in Fig. 5 to the presentation of individual *tones 1–8*. The gray scale represents the average number of spikes evoked by each tone over 25 trials. The tonotopic structure of the model is reflected by the shift, along the *x*-axis, of the tone that elicits the maximal response in each unit. *B*: enhancement/suppression of the Ex units in response to paired tones when the 2nd tone is Tn4, at different ISIs (*top*, *middle*, and *bottom*). The colors of the vertical lines indicate an average increase (enhancement, blue) or decrease (suppression, red) in the number of spikes in response to Tn4 preceded by each of the 8 tones (*y*-axis), compared with the response to a solitary Tn4. In all simulations, each Ex (Inh) unit received independent noise input with i_{noise_Ex} (i_{noise_Inh}) set to 0.04 nA (0.025 nA).
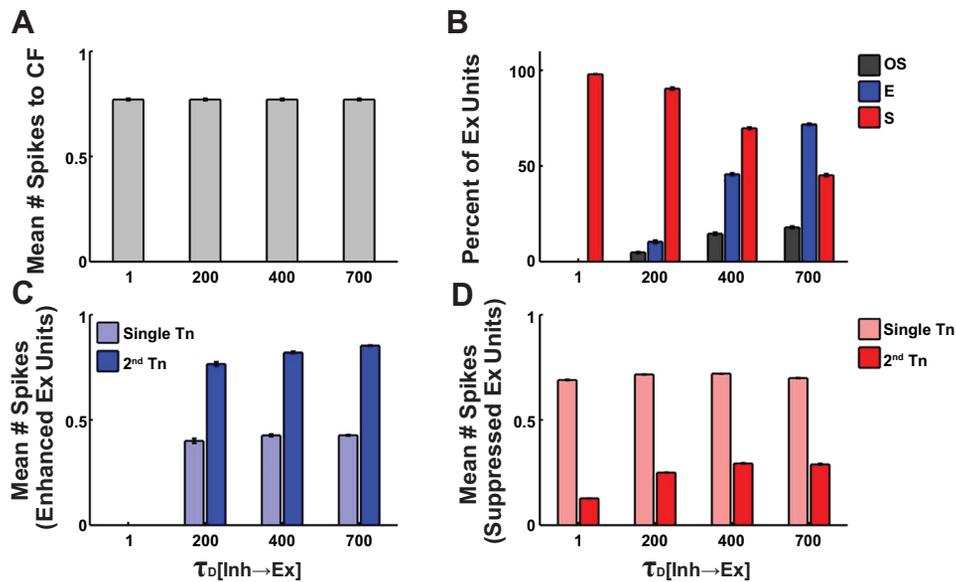
Fig. 7. Experimental variability of order-sensitivity can be explained by long-term plasticity of the temporal profile of Inh→Ex PPD. *A*: mean number of spikes over all Ex units in response to their respective CF at each tested regime for the PPD of IPSPs (τ_D of the Inh→Ex synapses set to 1, 200, 400 and 700 ms). *B*: % of Ex units exhibiting order-selectivity (OS), heteroenhancement (E), and homosuppression (S) at a 100-ms ISI, for each τ_D value. Order-selectivity and heteroenhancement were measured for all 16 neighboring tone pairs, while homosuppression was measured for the 8 homotone pairs. Each unit was classified as exhibiting an order-selective, enhanced, or suppressed response by χ^2-test at the 1% significance level, based on its responses over 25 trials. No heteroenhanced (or order selective) responses were observed to any of the tone pairs when PPD of the IPSPs was absent ($\tau_D = 1$). *C*: increase in the mean number of spikes in heteroenhancement units (as defined in *B*) in response to the 2nd tone of the preferred tone pair at a 100-ms ISI, compared with the response to that tone when presented in isolation. *D*: decrease in the mean number of spikes in homosuppression units in response to the 2nd tone at a 100-ms ISI, compared with the response to the tone when presented in isolation. In all panels, bars represent mean values over 5 replications of 1,000-unit networks, and error bars indicate SE of this mean. In all simulations, each Ex (Inh) unit received independent noise input with $i_{\text{noise\_Ex}}$ ($i_{\text{noise\_Inh}}$) set to 0.04 nA (0.025 nA).

prevalence of heteroenhancement but also its robustness. Additionally, Fig. 7*D* shows that the magnitude of homosuppression in the units that exhibited statistically suppressed responses decreased as the PPD of IPSPs increased (significant interaction between τ_D[Inh→Ex] and suppression, $F_{3,32} = 543$, $P < 10^{-10}$), confirming a decreased robustness of homosuppression.

To examine the generality of the above results we also examined order-selectivity and order-sensitivity across different network sizes. In these simulations we increased the number of units while maintaining the connection probabilities and total synaptic inputs to each unit constant. With τ_D of the Inh→Ex synapses set to 700 ms and the ISI set to 100 ms, a 2,000-unit model of A1 produced 20.7% order-selective units while a 4,000-unit model produced 17.4% order-selective units (compared with 17.9% in the 1,000-unit model), demonstrating that the presence of order-selective units is robust across a range of different network sizes.

As a further test of the generality of the model we examined the effects of stimulus intensity on order-tuning. We mirrored the protocol of Brosch and Schreiner (1997, 2000), where the intensity of the second tone was kept constant while the intensity of the first tone was varied. Results from these and other studies (Sadagopan and Wang 2009) reveal that stimulus intensity affects order-sensitivity in a complex manner on a cell-by-cell basis. We modeled changes in stimulus intensity by varying the number of Input units activated by each tone (see MATERIALS AND METHODS), reproducing the standard expansion of the spectral receptive field of cortical neurons when stimulus intensity increases. Simulations of the 1,000-unit model under varying intensities of the first tone, with the stimulus intensity of the second tone held at *level 3*, revealed a

nonlinear relationship between the stimulus intensity and both heteroenhancement and order-selectivity (Fig. 8). Very low intensities did not produce much order-selectivity, and a level-dependent increase in selectivity plateaued at *levels 3–5* (Fig.
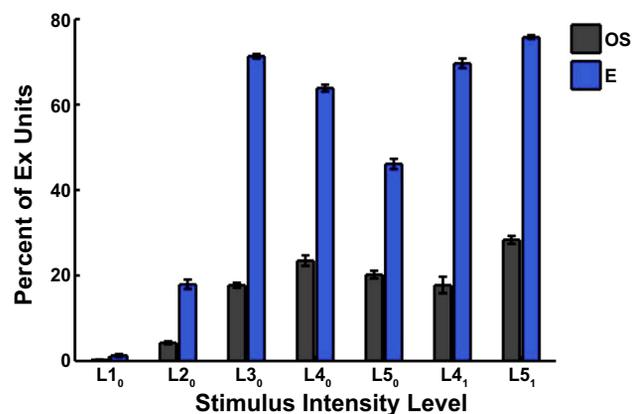

Fig. 8. Stimulus intensity affects order-tuning in a nonlinear manner: % of Ex units exhibiting order-selectivity (OS) and heteroenhancement (E) for each instance of the stimulus intensity protocol Lx_y, where *x* represents the intensity level of the 1st tone and *y* represents the number of tones separating the 1st and 2nd tones in each pair ("frequency distance"). In these simulations, τ_D of the Inh→Ex synapses was 700 ms and stimuli pairs were presented at a 100-ms ISI. Units were classified as order-selective and/or heteroenhanced as in Fig. 7*B*. Heteroenhanced and order-selective responses increased with the intensity of the 1st stimulus. However, at higher intensities, order-selective responses plateaued while heteroenhanced responses decreased. Moreover, at higher intensities an increase in enhancement was observed when the tone frequencies of the stimulus pair were farther apart. Bars represent mean values over 5 replications of 1,000-unit networks, and error bars indicate SE. In all simulations, each Ex (Inh) unit received independent noise input with $i_{\text{noise\_Ex}}$ ($i_{\text{noise\_Inh}}$) set to 0.04 nA (0.025 nA).

8, gray bars). Enhancement displayed a similar pattern, although there was a decrease at *level 5* ($L5_0$, where the subscript refers to the frequency distance between the tones in the pair) compared with *level 4* ($L4_0 \times L5_0$, $t_8 = 12$, $P < 10^{-5}$); however, there was an effect of the frequency distance between the tones in a pair. For example, at high intensities (*level 5*) more units exhibited enhancement at $L5_1$ compared with $L5_0$ ($t_8 = 23$, $P < 10^{-6}$). Therefore, these results reveal that order-tuning interacted in a complex fashion with intensity, a finding consistent with the experimental data.

DISCUSSION

PPD of IPSPs is a universally observed form of short-term plasticity at synapses from parvalbumin-positive/fast-spiking inhibitory neurons (Buonomano and Merzenich 1998; Chance et al. 2002; Gupta et al. 2000; Holmgren et al. 2003; Kapfer et al. 2007; Ma et al. 2012; Nathan and Lambert 1991; Reyes 2011). However, the computational role of short-term depression of IPSPs is not known. Here we propose that a primary computational function of PPD of IPSPs may be to contribute to order-selectivity.

Computational Function of STP at Different Synapses

Since Eccles et al. (1941) first described STP at the neuromuscular junction over 60 years ago, hundreds of studies have demonstrated that synaptic efficacy is not constant but changes dramatically over the course of hundreds of milliseconds in a use-dependent fashion (Abbott and Regehr 2004; Zucker 1989; Zucker and Regehr 2002). Indeed, every class of cortical synapses studied to date exhibits some form of STP. But despite its ubiquity, and in sharp contrast to long-term forms of plasticity, there is no generally accepted computational role for STP. On theoretical grounds STP has been proposed to contribute to a number of different functions including temporal processing (Buonomano 2000; Buonomano and Merzenich 1995; Fortune and Rose 2001), gain control (Abbott et al. 1997; Chance et al. 1998; Rothman et al. 2009), network stability (Galarreta and Hestrin 1998; Sussillo et al. 2007), and working memory (Hansel and Mato 2013; Maass and Markram 2002; Mongillo et al. 2008). Experimental studies over the past decade have provided significant support for the notion that STP underlies some forms of temporal selectivity. Specifically, interval-selective neurons in crickets, frogs, and electric fish seem to rely on STP (Carlson 2009; Goel and Buonomano 2014; Kostarakos and Hedwig 2012; Rose et al. 2011).

STP is, of course, not a single phenomenon; different synapse classes are characterized by different directions, magnitudes, and temporal profiles. However, it is important to stress that some of this variability may arise from differences in preparations, concentration of divalent cations, developmental state, and temperature (Crins et al. 2011; Klyachko and Stevens 2006; Kushmerick et al. 2006; Lorteije et al. 2009). Nevertheless, while the individual parameters of STP may vary, the forms of STP examined here are very robust and have been repeatedly observed in vivo in the cortex (Cohen-Kashi Malina et al. 2013; Wehr and Zador 2003). Part of the challenge in understanding the computational role of STP is deciphering whether the different forms of STP have functionally distinct roles or are closely intertwined. For example, does PPD of

IPSPs have the same function as PPF of EPSPs or a distinct computational function?

Here we have parametrically studied STP at three different synapse classes and demonstrated that it is the PPD of IPSPs, more so than the facilitation or depression of Ex→Ex and Ex→Inh synapses, that is central to order-selectivity. Specifically, in a reduced disynaptic network, depression of IPSPs was the only form of STP that was necessary for the generation of order-selective neurons. There are two primary reasons for this: *1*) inhibitory neurons serve as a required point of convergence between two distinct inputs, and *2*) PPD of IPSPs provides a memory of previous events, a memory that can be expressed through disinhibition of excitatory inputs. In contrast to previous models, here order-selectivity arises from canonical circuit properties and defined synaptic physiology, as opposed to customized circuits or hypothetical delay lines.

Paired-Tone Suppression, Enhancement, and Order-Selectivity in Vivo

Although many studies have reported order-sensitive and order-selective neurons in vivo (Bartlett and Wang 2005; Brosch et al. 1999; Kilgard and Merzenich 2002; Lewicki and Arthur 1996; Margoliash and Fortune 1992; Razak and Fuzessery 2009; Sadagopan and Wang 2009; Suga et al. 1978; Yin et al. 2008), the phenomena of paired-tone suppression and enhancement have been more widely examined. These studies have led to the emergence of some common themes: *1*) suppression is observed more often than enhancement (Brosch et al. 1999; Brosch and Schreiner 1997, 2000; Peng et al. 2010; Scholes et al. 2011; Tan et al. 2004; Wehr and Zador 2005); *2*) suppression is generally dominant when the first and second tones are of the same frequency ("homosuppression") and most pronounced at short intertone intervals (<50 ms) (Brosch et al. 1999; Brosch and Schreiner 1997, 2000; Peng et al. 2010; Scholes et al. 2011); and *3*) when enhancement is observed, it generally occurs at longer intervals (≅100 ms) and when the first and second tones are of different frequencies ("heteroenhancement") (Brosch et al. 1999; Brosch and Schreiner 2000; Peng et al. 2010; Scholes et al. 2011).

Intracellular studies have suggested that homosuppression of auditory tones is largely a result of two factors: *1*) GABAergic inhibition produced by the first tone that is still present at the time of the second (Tan et al. 2004; Wehr and Zador 2005) and *2*) PPD of EPSPs that are driving the tone responses (Wehr and Zador 2005). There is also evidence, however, that homosuppression involves intrinsic bursting properties of thalamocortical projection neurons (Bayazitov et al. 2013).

Here we propose that order-selectivity and paired-tone enhancement are, in part, a result of the disinhibition produced by PPD of IPSPs. This hypothesis shares some similarities with previous models of order-selectivity (Brosch and Schreiner 2000; Drew and Abbott 2003). However, an important distinction is that unlike the notion in which inhibitory neurons may be inhibited by the first event, thus disinhibiting the second event, here disinhibition is "hidden"—that is, it cannot be observed by increased spontaneous firing rates following the first tone—and the firing of inhibitory neurons is not directly inhibited.

The mechanisms we propose are consistent with a recent report of homoenhancement (postadaptation facilitation) in the

barrel cortex (Cohen-Kashi Malina et al. 2013). That study demonstrated that after a brief train of principal whisker stimulation, a subsequent test stimulus can produce an enhanced response. The authors go on to show that this facilitation (which was not present in the thalamus) is likely accounted for by the PPD of IPSPs, as opposed to PPF of excitatory synapses.

Experimental Predictions

One clear experimental prediction that arises from the parametric study in Fig. 4 is that among the forms of STP at different synapses PPD of IPSPs is the most important for order-selectivity. Thus some forms of auditory order-selectivity should be significantly impaired by blocking short-term depression of IPSPs from the fast-spiking (parvalbumin positive) inhibitory neurons. It remains technically challenging to specifically alter short-term depression of these cells, that is, to prevent depression of the second IPSP without altering the first IPSP, or "baseline" inhibition—this of course is a serious concern since the definition of order-selectivity is in part based on the response to the first event. A less powerful, but less challenging approach would be to inactivate parvalbumin-positive neurons during stimulus presentation. Recent optogenetic studies have done this by using optogenetic methods to suppress parvalbumin-positive inhibitory neurons in the auditory and visual cortex (Li et al. 2013; Lien and Scanziani 2013). These studies produced dramatic changes in response to a single sensory event (and thus do not allow one to make direct conclusions about order-selectivity under baseline conditions) and reported that direction-selectivity was mostly preserved. Thus, in these studies, the observed direction-selectivity appeared to primarily originate from subcortical areas—a finding consistent with the fact that direction-selectivity in the visual system likely relies on subcortical mechanisms (Elstrott and Feller 2009). Other results suggest that activating parvalbumin-positive neurons might alter highly direction-selective neurons in the visual cortex (e.g., Fig. S8 of Wilson et al. 2012). To date, however, no studies have directly examined the effects of parvalbumin-positive inhibitory neurons on order-selectivity in the auditory cortex.

A further prediction emerges from the reported variation in the percentage of auditory neurons that exhibit suppression, enhancement, and order-selectivity. While most studies report that paired-tone suppression is most commonly observed, some studies report a large number of cells that exhibit enhancement in response to tone pairs or sequences. It is clear, however, that the percentage of order-sensitive neurons should not be seen as a hardwired property of the auditory cortex but as an experience-dependent property altered by cortical plasticity. That is, primary cortical areas seem to undergo forms of plasticity that increase the representation of temporally selective neurons. Indeed, many of the studies that have characterized order-selective and complex spatiotemporally selective neurons in vertebrates have done so in animals trained on sequences of tones or other complex auditory stimuli (Engineer et al. 2008; Kilgard and Merzenich 1999, 2002; Yin et al. 2008). Here we propose that the experience-dependent shifts in the percentage of order-sensitive and enhancement neurons is due to changes in short-term plasticity—a phenomenon that has been referred to as metaplasticity of short-term plasticity (Carvalho and Buonomano 2011). Specifically, we predict that experience-dependent forms of learning that increase the percentage of order-selective neurons should produce a detectable mean increase in the PPD of IPSPs.

Many in vivo auditory studies suggest that order-selectivity and order-sensitivity arise in the cortex. For example, studies reveal significant qualitative differences between in vivo thalamic and cortical responses to consecutive pulses and suggest that certain forms of paired-tone suppression, enhancement, and order-selectivity are cortical phenomena (Bayazitov et al. 2013; Brosch and Schreiner 1997; Creutzfeldt et al. 1980; Miller et al. 2002; Razak and Fuzessery 2009; Wang et al. 1995; Wehr and Zador 2005). Here we hypothesize that STP is a crucial mechanism underlying order-selectivity and order-sensitivity in the auditory cortex. At the same time, we stress that, given the universal importance of order-selectivity (and direction-selectivity) across animals, timescales, and sensory modalities, the nervous system likely evolved multiple different mechanisms for order-selectivity. Particularly in subcortical circuits, delay-line and rebound excitation mechanisms also contribute to order- and interval-selectivity over a range of different timescales (Carr 1993; Elstrott and Feller 2009; Jeffress 1948; Suga et al. 1983).

Conclusions

Here we propose that STP may underlie some forms of cortically generated order-selectivity. In contrast to previous models, in the present framework order-selectivity can be observed in a minimal circuit of two neurons, based entirely on known cellular and synaptic properties, without the need to invoke delay lines, or circuits tuned through experience-dependent plasticity—which is not to say these additional mechanisms might not also contribute to order-selectivity. One specific prediction that is made is that among the different types of STP present at excitatory and inhibitory synapses, PPD of the IPSP is the most important for order-selectivity.

DISCLOSURES

No conflicts of interest, financial or otherwise, are declared by the author(s).

AUTHOR CONTRIBUTIONS

Author contributions: V.G. performed experiments; V.G. analyzed data; V.G. and D.V.B. interpreted results of experiments; V.G. and D.V.B. prepared figures; V.G. and D.V.B. drafted manuscript; V.G. and D.V.B. edited and revised manuscript; V.G. and D.V.B. approved final version of manuscript; D.V.B. conception and design of research.

REFERENCES

Abbott LF, Regehr WG. Synaptic computation. *Nature* 431: 796–803, 2004.
Abbott LF, Varela JA, Sen K, Nelson SB. Synaptic depression and cortical gain control. *Science* 275: 220–224, 1997.

Atencio CA, Schreiner CE. Spectrotemporal processing differences between auditory cortical fast-spiking and regular-spiking neurons. *J Neurosci* 28: 3897–3910, 2008.

Barlow HB, Levick WR. The mechanism of directionally selective units in rabbit's retina. *J Physiol* 178: 477–504, 1965.

Bartlett EL, Wang X. Long-lasting modulation by stimulus context in primate auditory cortex. *J Neurophysiol* 94: 83–104, 2005.

Bayazitov IT, Westmoreland JJ, Zakharenko SS. Forward suppression in the auditory cortex is caused by the Ca$_v$3.1 calcium channel-mediated switch from bursting to tonic firing at thalamocortical projections. *J Neurosci* 33: 18940–18950, 2013.

Brosch M, Schreiner CE. Time course of forward masking tuning curves in cat primary auditory cortex. *J Neurophysiol* 77: 923–943, 1997.

Brosch M, Schreiner CE. Sequence sensitivity of neurons in cat primary auditory cortex. *Cereb Cortex* 10: 1155–1167, 2000.

Brosch M, Schulz A, Scheich H. Processing of sound sequences in macaque auditory cortex: response enhancement. *J Neurophysiol* 82: 1542–1559, 1999.

Buonomano DV. Decoding temporal information: a model based on short-term synaptic plasticity. *J Neurosci* 20: 1129–1141, 2000.

Buonomano DV, Merzenich MM. Temporal information transformed into a spatial code by a neural network with realistic properties. *Science* 267: 1028–1030, 1995.

Buonomano DV, Merzenich MM. Net interaction between different forms of short-term synaptic plasticity and slow-IPSPs in the hippocampus and auditory cortex. *J Neurophysiol* 80: 1765–1774, 1998.

Byrnes S, Burkitt AN, Grayden DB, Meffin H. Learning a sparse code for temporal sequences using STDP and sequence compression. *Neural Comput* 23: 2567–2598, 2011.

Carlson BA. Temporal-pattern recognition by single neurons in a sensory pathway devoted to social communication behavior. *J Neurosci* 29: 9417–9428, 2009.

Carr CE. Processing of temporal information in the brain. *Annu Rev Neurosci* 16: 223–243, 1993.

Carvalho TP, Buonomano DV. Differential effects of excitatory and inhibitory plasticity on synaptically driven neuronal input-output functions. *Neuron* 61: 774–785, 2009.

Carvalho TP, Buonomano DV. A novel learning rule for long-term plasticity of short-term synaptic plasticity enhances temporal processing. *Front Integr Neurosci* 5: 20, 2011.

Chance FS, Abbott LF, Reyes AD. Gain modulation from background synaptic input. *Neuron* 35: 773–782, 2002.

Chance FS, Nelson SB, Abbott LF. Synaptic depression and the temporal response characteristics of V1 cells. *J Neurosci* 18: 4785–4799, 1998.

Cheetham CE, Fox K. The role of sensory experience in presynaptic development is cortical area-specific. *J Physiol* 589: 5691–5699, 2011.

Cheetham CE, Hammond MS, Edwards CE, Finnerty GT. Sensory experience alters cortical connectivity and synaptic function site specifically. *J Neurosci* 27: 3456–3465, 2007.

Cohen-Kashi Malina K, Jubran M, Katz Y, Lampl I. Imbalance between excitation and inhibition in the somatosensory cortex produces postadaptation facilitation. *J Neurosci* 33: 8463–8471, 2013.

Creutzfeldt O, Hellweg FC, Schreiner C. Thalamo-cortical transformation of responses to complex auditory stimuli. *Exp Brain Res* 39: 87–104, 1980.

Crins TT, Rusu SI, Rodriguez-Contreras A, Borst JG. Developmental changes in short-term plasticity at the rat calyx of Held synapse. *J Neurosci* 31: 11706–11717, 2011.

Daw MI, Ashby MC, Isaac JT. Coordinated developmental recruitment of latent fast spiking interneurons in layer IV barrel cortex. *Nat Neurosci* 10: 453–461, 2007.

Dehaene S, Changeux JP, Nadal JP. Neural networks that learn temporal sequences by selection. *Proc Natl Acad Sci USA* 84: 2727–2731, 1987.

Deisz RA. The GABA$_B$ receptor antagonist CGP 55845A reduces presynaptic GABA$_B$ actions in neocortical neurons of the rat in vitro. *Neuroscience* 93: 1241–1249, 1999.

Destexhe A, Mainen ZF, Sejnowski TJ. An efficient method for computing synaptic conductances based on a kinetic model of receptor binding. *Neural Comput* 6: 14–18, 1994.

Doupe AJ. Song- and order-selective neurons in the songbird anterior forebrain and their emergence during vocal development. *J Neurosci* 17: 1147–1167, 1997.

Doupe AJ, Kuhl PK. Birdsong and human speech: common themes and mechanisms. *Annu Rev Neurosci* 22: 567–631, 1999.

Drew PJ, Abbott LF. Model of song selectivity and sequence generation in area HVc of the songbird. *J Neurophysiol* 89: 2697–2706, 2003.

Eccles JC, Katz B, Kuffler SW. Nature of the "endplate potential" in curarized muscle. *J Neurophysiol* 4: 362–387, 1941.

Elstrott J, Feller MB. Vision and the establishment of direction-selectivity: a tale of two circuits. *Curr Opin Neurobiol* 19: 293–297, 2009.

Engineer CT, Perez CA, Chen YH, Carraway RS, Reed AC, Shetake JA, Jakkamsetti V, Chang KQ, Kilgard MP. Cortical activity patterns predict speech discrimination ability. *Nat Neurosci* 11: 603–608, 2008.

Finnerty GT, Connors BW. Sensory deprivation without competition yields modest alterations of short-term synaptic dynamics. *Proc Natl Acad Sci USA* 97: 12864–12868, 2000.

Fortune ES, Rose GJ. Short-term synaptic plasticity as a temporal filter. *Trends Neurosci* 24: 381–385, 2001.

Gabernet L, Jadhav SP, Feldman DE, Carandini M, Scanziani M. Somatosensory integration controlled by dynamic thalamocortical feed-forward inhibition. *Neuron* 48: 315–327, 2005.

Galarreta M, Hestrin S. Frequency-dependent synaptic depression and the balance of excitation and inhibition in the neocortex. *Nat Neurosci* 1: 587–594, 1998.

Goel A, Buonomano DV. Timing as an intrinsic property of neural networks: evidence from in vivo and in vitro experiments. *Philos Trans R Soc Lond B Biol Sci* 369: 20120460, 2014.

Gonchar Y, Burkhalter A. Three distinct families of GABAergic neurons in rat visual cortex. *Cereb Cortex* 7: 347–358, 1997.

Gupta A, Wang Y, Markram H. Organizing principles for a diversity of GABAergic interneurons and synapses in the neocortex. *Science* 287: 273–278, 2000.

Hansel D, Mato G. Short-term plasticity explains irregular persistent activity in working memory tasks. *J Neurosci* 33: 133–149, 2013.

Hines ML, Carnevale NT. The NEURON simulation environment. *Neural Comput* 9: 1179–1209, 1997.

Hirsh IJ. Auditory perception of temporal order. *J Acoust Soc Am* 31: 759–767, 1959.

Holmgren C, Harkany T, Svennenfors B, Zilberter Y. Pyramidal cell communication within local networks in layer 2/3 of rat neocortex. *J Physiol* 551: 139–153, 2003.

Hooper SL, Buchman E, Hobbs KH. A computational role for slow conductances: single-neuron models that measure duration. *Nat Neurosci* 5: 552–556, 2002.

Hull C, Isaacson JS, Scanziani M. Postsynaptic mechanisms govern the differential excitation of cortical neurons by thalamic inputs. *J Neurosci* 29: 9127–9136, 2009.

Jeffress LA. A place theory of sound localization. *J Comp Physiol Psychol* 41: 35–39, 1948.

Kanold PO, Manis PB. Encoding the timing of inhibitory inputs. *J Neurophysiol* 93: 2887–2897, 2005.

Kapfer C, Glickfeld LL, Atallah BV, Scanziani M. Supralinear increase of recurrent inhibition during sparse activity in the somatosensory cortex. *Nat Neurosci* 10: 743–753, 2007.

Kawaguchi Y, Kubota Y. GABAergic cell subtypes and their synaptic connections in rat frontal cortex. *Cereb Cortex* 7: 476–486, 1997.

Kilgard MP, Merzenich MM. Distributed representation of spectral and temporal information in rat primary auditory cortex. *Hear Res* 134: 16–28, 1999.

Kilgard MP, Merzenich MM. Order-sensitive plasticity in adult primary auditory cortex. *Proc Natl Acad Sci USA* 99: 3205–3209, 2002.

Klyachko VA, Stevens CF. Temperature-dependent shift of balance among the components of short-term plasticity in hippocampal synapses. *J Neurosci* 26: 6945–6957, 2006.

Kostarakos K, Hedwig B. Calling song recognition in female crickets: temporal tuning of identified brain neurons matches behavior. *J Neurosci* 32: 9601–9612, 2012.

Kubota JT, Banaji MR, Phelps EA. The neuroscience of race. *Nat Neurosci* 15: 940–948, 2012.

Kushmerick C, Renden R, von Gersdorff H. Physiological temperatures reduce the rate of vesicle pool depletion and short-term depression via an acceleration of vesicle recruitment. *J Neurosci* 26: 1366–1377, 2006.

Lambert NA, Wilson WA. Temporally distinct mechanisms of use-dependent depression at inhibitory synapses in the rat hippocampus in vitro. *J Neurophysiol* 72: 121–130, 1994.

Lee TP, Buonomano DV. Unsupervised formation of vocalization-sensitive neurons: a cortical model based on short-term and homeostatic plasticity. *Neural Comput* 24: 2579–2603, 2012.

Levy RB, Reyes AD. Spatial profile of excitatory and inhibitory synaptic connectivity in mouse primary auditory cortex. *J Neurosci* 32: 5609–5619, 2012.

Lewicki MS, Arthur BJ. Hierarchical organization of auditory temporal context sensitivity. *J Neurosci* 16: 6987–6998, 1996.

Lewicki MS, Konishi M. Mechanisms underlying the sensitivity of songbird forebrain neurons to temporal order. *Proc Natl Acad Sci USA* 92: 5582–5586, 1995.

Li LY, Li YT, Zhou M, Tao HW, Zhang LI. Intracortical multiplication of thalamocortical signals in mouse auditory cortex. *Nat Neurosci* 16: 1179–1181, 2013.

Li LY, Xiong XR, Ibrahim LA, Yuan W, Tao HW, Zhang LI. Differential receptive field properties of parvalbumin and somatostatin inhibitory neurons in mouse auditory cortex. *Cereb Cortex* (January 14, 2014). doi: 10.1093/cercor/bht417.

Lien AD, Scanziani M. Tuned thalamic excitation is amplified by visual cortical circuits. *Nat Neurosci* 16: 1315–1323, 2013.

Lorteije JA, Rusu SI, Kushmerick C, Borst JG. Reliability and precision of the mouse calyx of Held synapse. *J Neurosci* 29: 13770–13784, 2009.

Lu JT, Li CY, Zhao JP, Poo MM, Zhang XH. Spike-timing-dependent plasticity of neocortical excitatory synapses on inhibitory interneurons depends on target cell type. *J Neurosci* 27: 9711–9720, 2007.

Ma Y, Hu H, Agmon A. Short-term plasticity of unitary inhibitory-to-inhibitory synapses depends on the presynaptic interneuron subtype. *J Neurosci* 32: 983–988, 2012.

Maass W, Markram H. Synapses as dynamic memory buffers. *Neural Netw* 15: 155–161, 2002.

Marder CP, Buonomano DV. Timing and balance of inhibition enhance the effect of long-term potentiation on cell firing. *J Neurosci* 24: 8873–8884, 2004.

Margoliash D, Fortune ES. Temporal and harmonic combination-sensitive neurons in the zebra finch's HVc. *J Neurosci* 12: 4309–4326, 1992.

Markram H, Wang Y, Tsodyks M. Differential signaling via the same axon of neocortical pyramidal neurons. *Proc Natl Acad Sci USA* 95: 5323–5328, 1998.

McCormick DA, Connors BW, Lighthall JW, Prince DA. Comparative electrophysiology of pyramidal and sparsely spiny stellate neurons of the neocortex. *J Neurophysiol* 54: 782–806, 1985.

McCormick DA, Wang Z, Huguenard J. Neurotransmitter control of neocortical neuronal activity and excitability. *Cereb Cortex* 3: 387–398, 1993.

Metherate R, Ashe JH. Facilitation of an NMDA receptor-mediated EPSP by paired-pulse stimulation in rat neocortex via depression of GABAergic IPSPs. *J Physiol* 481: 331–348, 1994.

Miles R. Variation in strength of inhibitory synapses in the CA3 region of guinea-pig hippocampus in vitro. *J Physiol* 431: 659–676, 1990.

Miller LM, Escabi MA, Read HL, Schreiner CE. Spectrotemporal receptive fields in the lemniscal auditory thalamus and cortex. *J Neurophysiol* 87: 516–527, 2002.

Mongillo G, Barak O, Tsodyks M. Synaptic theory of working memory. *Science* 319: 1543–1546, 2008.

Moore AK, Wehr M. Parvalbumin-expressing inhibitory interneurons in auditory cortex are well-tuned for frequency. *J Neurosci* 33: 13713–13723, 2013.

Mossbridge JA, Fitzgerald MB, O'Connor ES, Wright BA. Perceptual-learning evidence for separate processing of asynchrony and order tasks. *J Neurosci* 26: 12708–12716, 2006.

Nathan T, Lambert JD. Depression of the fast IPSP underlies paired-pulse facilitation in area CA1 of the rat hippocampus. *J Neurophysiol* 66: 1704–1715, 1991.

Peng Y, Sun X, Zhang J. Contextual modulation of frequency tuning of neurons in the rat auditory cortex. *Neuroscience* 169: 1403–1413, 2010.

Pouille F, Scanziani M. Enforcement of temporal fidelity in pyramidal cells by somatic feed-forward inhibition. *Science* 293: 1159–1163, 2001.

Razak KA, Fuzessery ZM. GABA shapes selectivity for the rate and direction of frequency-modulated sweeps in the auditory cortex. *J Neurophysiol* 102: 1366–1378, 2009.

Reichardt W. Autocorrelation, a principle for the evaluation of sensory information by the central nervous system. In: *Sensory Communication*, edited by Rosenblith WA. Cambridge, MA: MIT Press, 1961, p. 303–317.

Reyes A, Sakmann B. Developmental switch in the short-term modification of unitary EPSPs evoked in layer 2/3 and layer 5 pyramidal neurons of rat neocortex. *J Neurosci* 19: 3827–3835, 1999.

Reyes AD. Synaptic short-term plasticity in auditory cortical circuits. *Hear Res* 279: 60–66, 2011.

Rose G, Leary C, Edwards C. Interval-counting neurons in the anuran auditory midbrain: factors underlying diversity of interval tuning. *J Comp Physiol A Neuroethol Sens Neural Behav Physiol* 197: 97–108, 2011.

Rothman JS, Cathala L, Steuber V, Silver RA. Synaptic depression enables neuronal gain control. *Nature* 1015–1018, 2009.

Rudy B, Fishell G, Lee S, Hjerling-Leffler J. Three groups of interneurons account for nearly 100% of neocortical GABAergic neurons. *Dev Neurobiol* 71: 45–61, 2011.

Sadagopan S, Wang X. Nonlinear spectrotemporal interactions underlying selectivity for complex sounds in auditory cortex. *J Neurosci* 29: 11192–11202, 2009.

Scholes C, Palmer AR, Sumner CJ. Forward suppression in the auditory cortex is frequency-specific. *Eur J Neurosci* 33: 1240–1251, 2011.

Shepherd GM. *The Synaptic Organization of the Brain*. New York: Oxford Univ. Press, 1998.

Silberberg G, Markram H. Disynaptic inhibition between neocortical pyramidal cells mediated by Martinotti cells. *Neuron* 53: 735–746, 2007.

Simmons JA. Bats use a neuronally implemented computational acoustic model to form sonar images. *Curr Opin Neurobiol* 22: 311–319, 2012.

Suga N, O'Neill WE, Kujirai K, Manabe T. Specificity of combination-sensitive neurons for processing of complex biosonar signals in auditory cortex of the mustached bat. *J Neurophysiol* 49: 1573–1626, 1983.

Suga N, O'Neill WE, Manabe T. Cortical neurons sensitive to combinations of information-bearing elements of biosonar signals in the mustache bat. *Science* 200: 778–781, 1978.

Sussillo D, Toyoizumi T, Maass W. Self-tuning of neural circuits through short-term synaptic plasticity. *J Neurophysiol* 97: 4079–4095, 2007.

Tallal P. Improving language and literacy is a matter of time. *Nat Rev Neurosci* 5: 721–728, 2004.

Tallal P, Piercy M. Defects of non-verbal auditory perception in children with developmental aphasia. *Nature* 241: 468–469, 1973.

Tan AY, Zhang LI, Merzenich MM, Schreiner CE. Tone-evoked excitatory and inhibitory synaptic conductances of primary auditory cortex neurons. *J Neurophysiol* 92: 630–643, 2004.

Tsodyks MV, Markram H. The neural code between neocortical pyramidal neurons depends on neurotransmitter release probability. *Proc Natl Acad Sci USA* 94: 719–723, 1997.

Wang L, Fontanini A, Maffei A. Experience-dependent switch in sign and mechanisms for plasticity in layer 4 of primary visual cortex. *J Neurosci* 32: 10562–10573, 2012.

Wang X, Merzenich MM, Beitel R, Schreiner CE. Representation of a species-specific vocalization in the primary auditory cortex of the common marmoset: temporal and spectral characteristics. *J Neurophysiol* 74: 2685–2706, 1995.

Wehr M, Zador AM. Balanced inhibition underlies tuning and sharpens spike timing in auditory cortex. *Nature* 426: 442–446, 2003.

Wehr M, Zador AM. Synaptic mechanisms of forward suppression in rat auditory cortex. *Neuron* 47: 437–445, 2005.

Wilson NR, Runyan CA, Wang FL, Sur M. Division and subtraction by distinct cortical inhibitory networks in vivo. *Nature* 488: 343–348, 2012.

Yin P, Mishkin M, Sutter M, Fritz JB. Early stages of melody processing: stimulus-sequence and task-dependent neuronal activity in monkey auditory cortical fields A1 and R. *J Neurophysiol* 100: 3009–3029, 2008.

Zhou X, de Villers-Sidani É, Panizzutti R, Merzenich MM. Successive-signal biasing for a learned sound sequence. *Proc Natl Acad Sci USA* 107: 14839–14844, 2010.

Zucker RS. Short-term synaptic plasticity. *Annu Rev Neurosci* 12: 13–31, 1989.

Zucker RS, Regehr WG. Short-term synaptic plasticity. *Annu Rev Physiol* 64: 355–405, 2002.